Electronic Supplementary Material (ESI) for Journal of Materials Chemistry B.

Supplementary data for

"Osteoimmune-Modulating and BMP-2 Eluting Anodised 3D Printed Titanium for Accelerated Bone Regeneration"

Masood Ali[1], Yan He[2], Anna Sze Ni Chang[3], Alice Wu[3], Jingyu Liu[4], Yuxue Cao[3], Yousuf Mohammad[1,3], Amirali Popat[3], Laurie Walsh[5], Qingsong Ye [6*], Chun Xu[5*], Tushar Kumeria[3,7*]

[1]Therapeutics Research Group, Frazer Institute, Faculty of Medicine, University of Queensland, Brisbane, QLD 4102, Australia

[2]Institute of Regenerative and Translational Medicine, Wuhan University of Science and Technology, Wuhan 430040, China

[3]School of Pharmacy, The University of Queensland, Brisbane, Queensland 4102, Australia

[4]School of Mechanical, Medical and process Engineering, Queensland University of Technology, Brisbane, Queensland 4000, Australia

[5]School of Dentistry, The University of Queensland, Herston, Queensland 4006, Australia

[6]Centre of Regenerative Medicine, Department of Stomatology, Renmin Hospital of Wuhan University, Wuhan 430060, China

[7]School of Materials Science and Engineering, University of New South Wales, Kensington, Sydney, New South Wales 2052, Australia

*Correspondence: t.kumeria@unsw.edu.au, chun.xu@uq.edu.au and qingsongye@whu.edu.cn

Table S1: List of Primers.

Primer sequence	Forward	Reverse
Inflammation/osteoclastogenic/fibrogenic gene markers		
IL1ra	5’-CTCCAGCTGGAGGAAGTTAAC-3’	5’-CTGACTCAAAGCTGGTGGTG-3’
TNFα	5’-CTGAACTTCGGGGTGATCGG-3’	5’-GGCTTGTCACTCGAATTTTGAGA-3’
IL1β	5’-TGGAGAGTGTGGATCCCAAG -3’	5’-GGTGCTGATGTACCAGTTGG -3’
CD86	5’- CTGCTCATCATTGTATGTCAC -3’	5’- ACTGCCTTCACTCTGCATTTG -3’
CD206	5’-AGACGAAATCCCTGCTACTG -3’	5’-CACCCATTCGAAGGCATTC -3’
IL-6	5’-ATAGTCCTTCCTACCCCAATTTCC-3’	5’-GATGAATTGGATGGTCTTGGTCC-3’
VEGF	5’-GTCCCATGAAGTGATCAAGTTC-3’	5’-TCTGCATGGTGATGTTGCTCTCTG-3’
IL18	5’-TGGCCGACTTCACTGTACAAC-3’	5-’TGGGGTTCACTGGCACTTTG-3’
TGFβ1	5'-CAGTACAGCAAGGTCCTTGC-3'	5'-ACGTAGTAGACGATGGGCAG-3'
BMP-2	5’-GCTCCACAAACGAGAAAAGC-3’	5’-AGCAAGGGGAAAAGGACACT-3’
WNT10B	5’-CCAGGTGGTAACGGAAAACC-3’	5’-TGCCCTCCAACAGGTCTTG -3’
Arginase	5’-GGAATCTGCATGGGCAACCTGTGT-3’	5’-AGGGTCTACGTCTCGCAAGCCA-3
GAPDH Universal	5’-AACTTTGGCATTGTGGAAGG-3’	5’- ACACATTGGGGGTAGGAACA-3’
Osteogenic gene markers		
OPN	5’-CCGGTGAAAGTGGCTGAGTT-3’	5’-TGCATGGTCTCCGTCGTCAT-3’
RUNX2	5’-TCT TTT GGG ATC CGA GCA CC-3’	5’-ATC TCC ACC ATG GTG CGG TT-3’
COL1A	5’-CCC CAA GGA GAA GAA GCA TG-3’	5’-GAA TCG ACT GTT GCC TTC GC-3’
IBSP	5’-GAG CAG CAC GGT TGA GTA TG-3’	5’-AGA CAG AAT GGG GAG TCC TC-3’
OCN	5’-GCC CTG ACT GCA TTC TGC CTC T-3’	5’-TCA CCA CCT TAC TGC CCT CCT G-3’

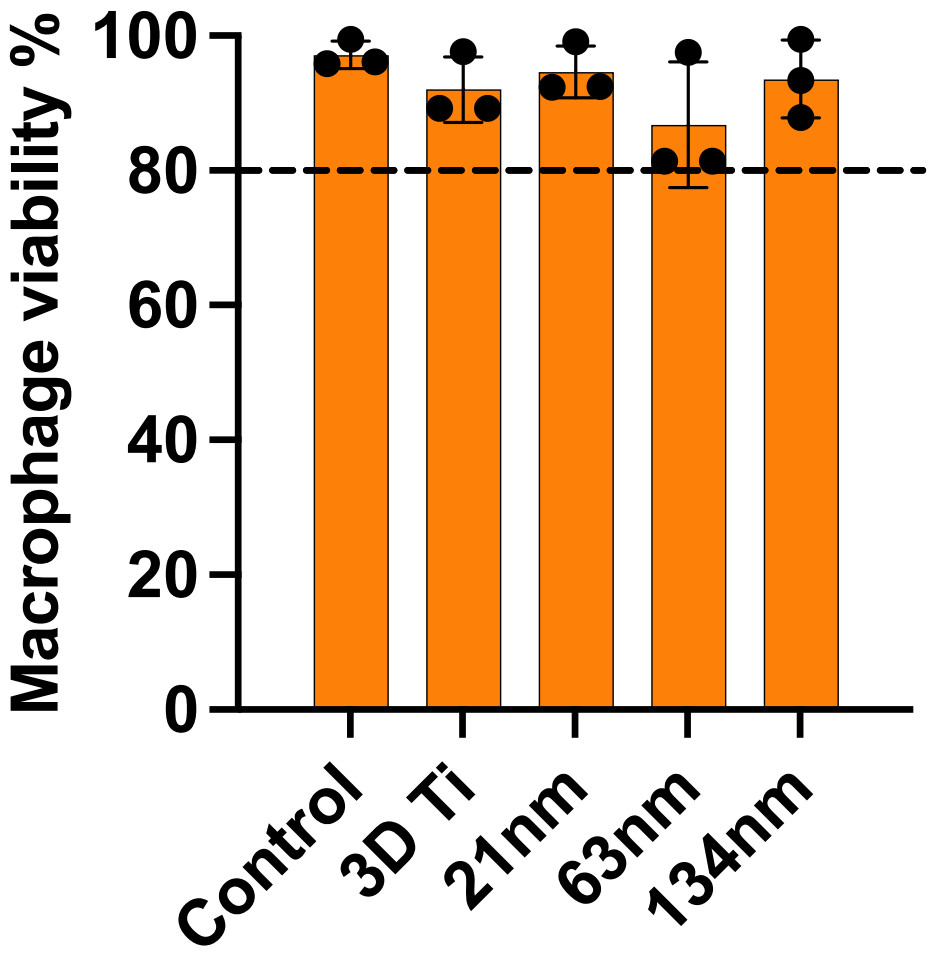

Figure S1: Macrophage cell viability studies on various pore diameter nanotubes. The data are presented relative to unstimulated macrophage cells (no LPS, no TiNTs). Control: Macrophage cells + LPS, Macrophage cells + LPS on 3D Ti surface and on 3D TiNTS with the following nanotube diameter; 21 nm, 63 nm, 134 nm. Data were calculated using PRISM.

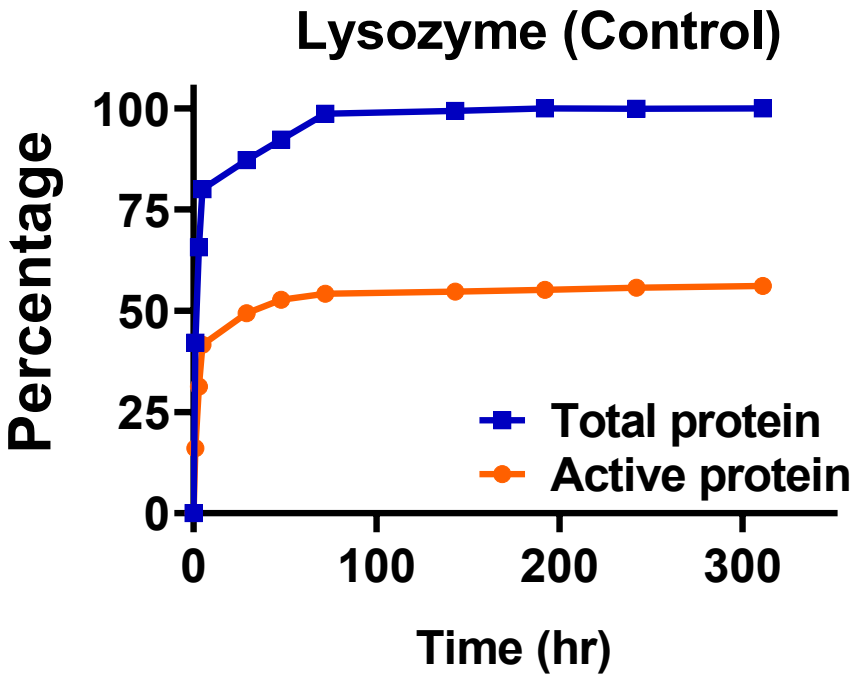

Figure S2: *In vitro* total and active lysozyme release from titanium nanotubes with 134nm diameter. Points on the blue curve represent the mean cumulative percentage of total amount of lysozyme released from the titanium nanotubes at various timepoints, quantified using BCA assay. Points on the respective excipient orange curves represents the mean cumulative percentage of active lysozyme released from the titanium nanotubes at various timepoints, quantified using Lyso activity assay. The bioactivity retention of the lysozyme was 56.13 ± 10.45 %. Data were calculated using PRISM. The error bars obtained from the standard deviations calculated in each set of the titanium nanotube discs showed that there was little inter-chip variability (n=3).

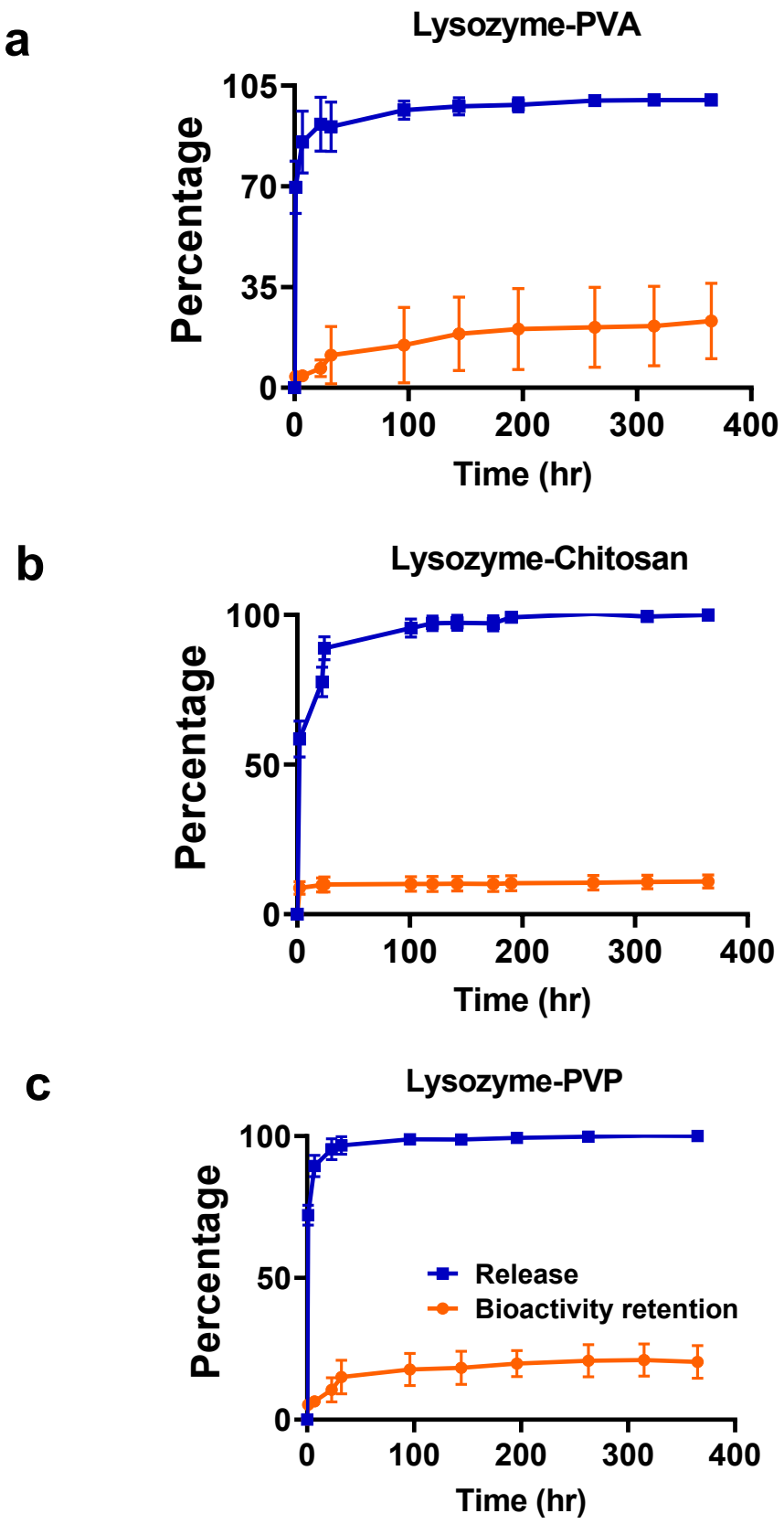

Figure S3: *In-vitro* total and active lysozyme release from TiNTs loaded with lysozyme in spiked with (a) Poly Vinyl alcohol (PVA), (b) Chitosan and (c) Poly Vinyl Pyrrolidone. Points

on the blue curve represents the mean cumulative percentage release of the total lysozyme amount release from the titanium nanotubes at various timepoints, quantified using BCA assay. Points on the respective excipient orange curves represent the mean cumulative percentage release of active lysozyme released from the titanium nanotubes at various timepoints, quantified using Lyso activity assay. The bioactivity retention of the spiked lysozyme was 23.22 ± 13.1 % for PVA, 10.99 ± 2.16 % for chitosan and 20.41 ± 5.80 % for PVP. Data were calculated using PRISM. The error bars obtained from the standard deviations calculated in each set of the titanium nanotube discs showed that there was little inter-chip variability (n=3).

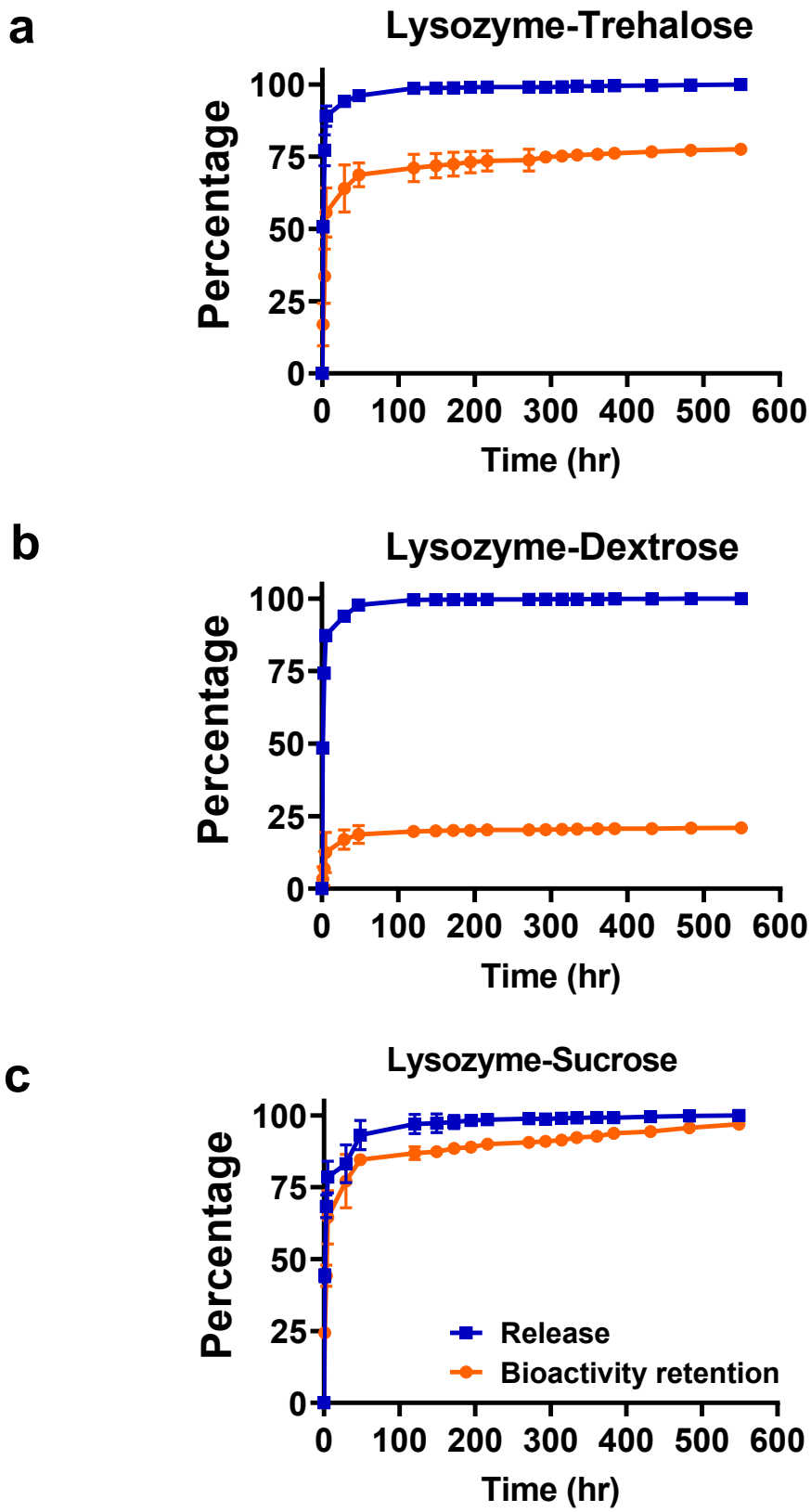

Figure S4: *In-vitro* total and active lysozyme release from TiNTs loaded with lysozyme in presence of (a) Trehalose, (b) Dextrose and (c) Sucrose. Points on the blue curve represent the mean cumulative percentage of total amount of lysozyme released from the Titanium

nanotubes at various timepoints, quantified using BCA assay. Points on the respective excipient orange curves represents the mean cumulative percentage of active lysozyme released from the titanium nanotubes at various timepoints, quantified using Lyso activity assay. The bioactivity retention of the spiked lysozyme was 77.56 ± 0.1 % for Trehalose, 20.95 ± 0.24 % for Dextrose and 96.93 ± 0.59 % for Sucrose. It was observed that sucrose had the highest bioactivity retention (96.93%), as the amount of its active and total lysozyme released were the closest. Data were calculated using PRISM. The error bars obtained from the standard deviations calculated in each set of the titanium nanotube discs showed that there was little inter-chip variability (n=3), suggesting that our methods have high reproducibility.

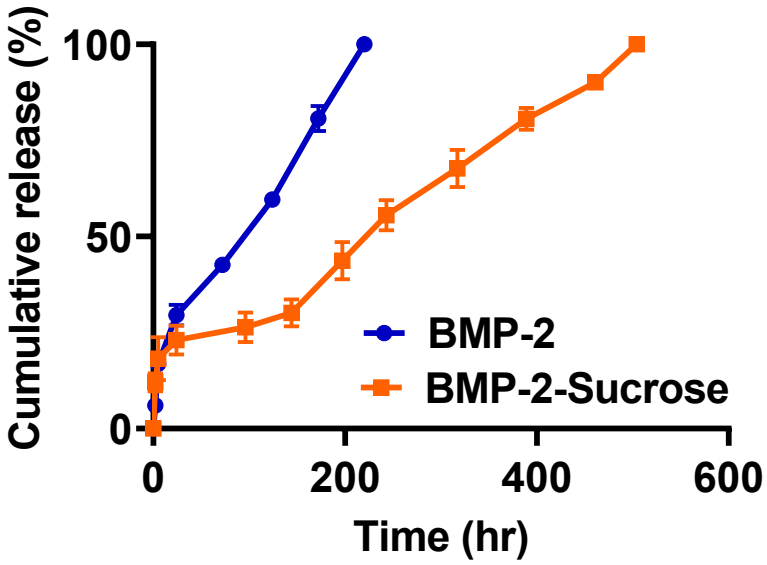

Figure S5: *In-vitro* release profile of BMP-2 and sucrose assisted BMP-2. BMP-2 released from TiNTs (134nm diameter) was better sustained for sucrose excipient protected samples compared to pure BMP-2 loaded (i.e. no excipient) TiNTs. Data were calculated using PRISM. The error bars obtained from the standard deviations calculated in each set of the titanium nanotubes showed that there was little inter-chip variability (n=3).